Electron structure and dynamics at poly(3-hexylthiophene)/fullerene photovoltaic heterojunctions

Zi Li, Xu Zhang, and Gang Lu[a)]
Department of Physics and Astronomy, California State University Northridge, California 91330-8268, USA

(Received 10 December 2010; accepted 5 February 2011; published online 25 February 2011)

The interfacial electronic structure and dynamics of poly(3-hexylthiophene)/fullerene (C_{60} and [6,6]-phenyl-C61-butyric acid methyl ester) heterojunctions are studied by *ab initio* nonadiabatic molecular dynamics. These junctions render ultrafast electron transfer with a time-scale of ~70 fs and the adiabatic electron transfer is the dominant process. The backward electron transfer, however, is much longer, in a time-scale of nanoseconds. The overall electron transfer is determined by the energy evolution driven by the coupled electron-ion dynamics. © *2011 American Institute of Physics*. [doi:10.1063/1.3559617]

The state-of-the-art of organic photovoltaics is so-called bulk heterojunction (BHJ) architecture[1,2] based on poly(3-hexylthiophene) (P3HT) and the fullerene derivative [6,6]-phenyl-C61-butyric acid methyl ester (PCBM), with efficiencies approaching 5%.[3,4] To further improve the efficiencies in such organic solar cells, however, progress has to be made in understanding fundamental electronic processes at the polymeric donors and the fullerene acceptors interface, which is the focus of this work. Fullerenes including PCBM and C_{60} are often used as the accepters because of their high electron affinity and high carrier mobility; as donors, P3HT has a band structure that matches reasonably well to that of the fullerenes and the solar spectrum. In BHJ solar cells, the interfacial electron transfer (ET) and electron-hole recombinations are extremely important, being the subject of intense research effort.[5–11] However, although atomic and electron structures of the interface have been investigated,[12–15] there is very little theoretical effort probing interfacial electron dynamics and in particular estimating ET rate. In addition, the mechanism of interfacial ET is yet to be clarified.

In this paper, we examine the electron structure and electron dynamics at the P3HT/fullerene interface using *ab initio* nonadiabatic (NA) molecular dynamics (MD) approach based on the Kohn–Sham (KS) ground state trajectory.[16–18] Specifically, the Ehrenfest dynamics of a photoexcited (PE) electron from the lowest-unoccupied-molecular-orbital (LUMO) of P3HT to the unoccupied states of fullerenes is characterized by the PE state expanded in terms of the KS ground states. The overall ET may be divided into NA and adiabatic contributions; both of them will be examined in this paper. To capture the stochastic nature of coupled electron-ion dynamics, 100 *ab initio* MD trajectories are averaged for the electron dynamics from a 1000 fs long MD simulation.[17–19] The *ab initio* MD is performed with the plane-wave pseudopotential approximation and the generalized gradient correction as implemented in the VASP code.[20,21] The gamma k-point is sampled with 400 eV energy cutoff in all calculations. The LUMO and the highest-occupied-molecular-orbital (HOMO) of P3HT are chosen from the relevant energy levels of the *entire* system that has the greatest localization at P3HT. Two different fullerenes are studied including C_{60} and PCBM. In addition, we have also examined Li-encapsulated C_{60}($Li@C_{60}$) to probe the doping effect on electron dynamics. The dimensions of the supercell are 16.20 Å × 15.67 Å × 13.15 Å, corresponding to a P3HT/PCBM mass density of 0.78 g/cm^3, slightly smaller than the experimental value of 1.1 g/cm^3. As shown in Fig. 1, at 0 K for all three junctions, P3HT HOMO lies in between the fullerenes' band gap, and P3HT LUMO is higher than the fullerenes' bottom three empty levels, making them the so-called type II heterojunctions.[13] In $P3HT/C_{60}$ and $P3HT/Li@C_{60}$, the fullerene levels are nearly degenerate owing to the higher symmetry of C_{60}. On the other hand, the energy levels split more in P3HT/PCBM with an additional state above the 4–6 levels of PCBM and the energy span of the four levels is 0.5 eV.

During the MD simulations at 300 K, although the fullerene structures remain more or less rigid, P3HT deforms significantly. In addition, the PE state distribution deviates significantly from that in the equilibrium structure. For example, at 0 K, the PE state is localized primarily on P3HT while at 300 K the PE state delocalizes to the fullerenes, forming a bridge state crossing the interface (Fig. 2). Moreover, the occupation fraction of the PE state on the fullerenes ranges from 0 to 0.6, and these delocalized PE state can facilitate the interfacial ET at 300 K. Among the three junctions, the PE state of $P3HT/Li@C_{60}$ is the most localized, while the PE state of P3HT/PCBM is the most delocalized,

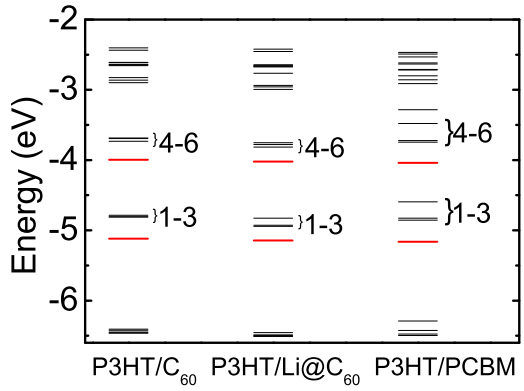

FIG. 1. (Color online) Energy diagrams of $P3HT/C_{60}$, $P3HT/Li@C_{60}$, and P3HT/PCBM junctions at 0 K. The lines below 1–3 and 4–6 indicate the HOMO and LUMO of P3HT. The low-lying empty levels of the fullerenes are indicated by numbers.

[a)]Electronic mail: ganglu@csun.edu.

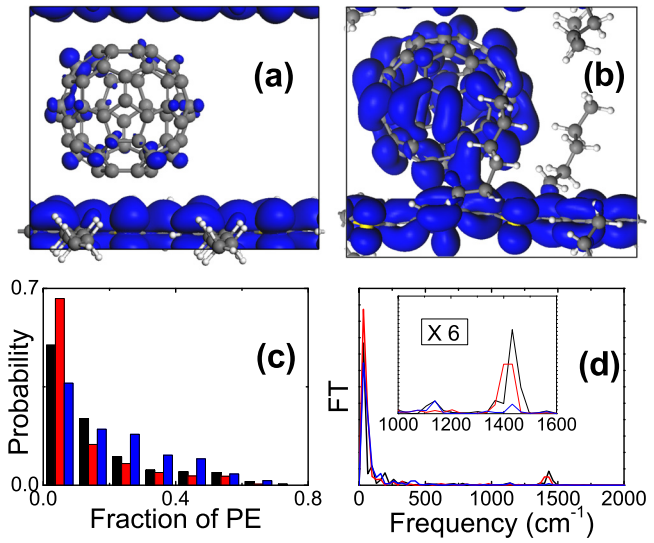

FIG. 2. (Color online) The PE state charge density of (a) P3HT/C_{60} equilibrium structure at 0 K and of (b) a snap shot during the MD simulations in which the fraction of the PE state on the fullerene is 0.59. The value of the isosurface is 0.001 e/Å^3. (c) The distribution of the occupation fraction of the PE state on the fullerene and (d) the FT of the PE state energy in P3HT/C_{60} (black), P3HT/Li@C_{60}, (red) and P3HT/PCBM (blue). The inset of (d) is a blown-up view (×6) at higher frequencies around 1400 cm^{-1}.

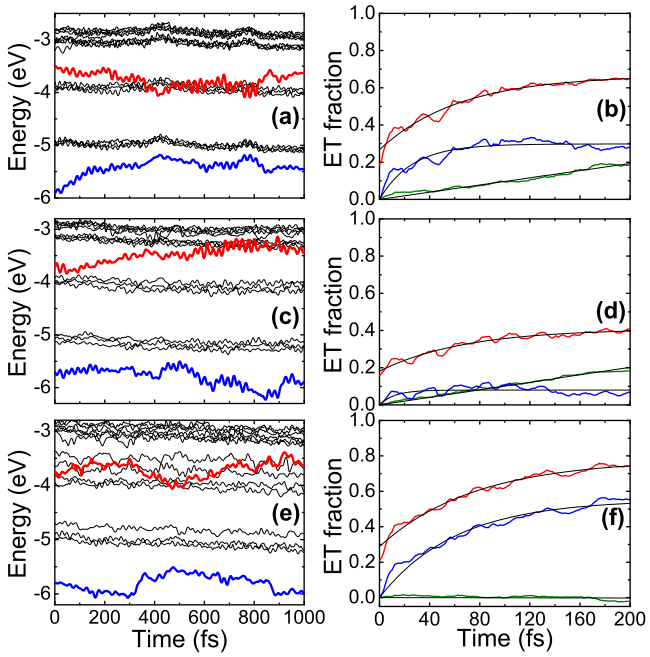

FIG. 3. (Color online) The time evolution of P3HT HOMO (lower thick blue), LUMO (upper thick red), and some low-lying fullerene conduction band levels (thin black curves) for (a) P3HT/C_{60}, (c) P3HT/Li@C_{60}, and (e) P3HT/PCBM junctions. The corresponding ET amount is displayed in (b), (d), and (f); the three curves in each figure from top to bottom correspond to the total (thick red), adiabatic (thick blue), and NA (thick green) contributions of ET. The thin black curves are the fits.

consistent with their respective electron dynamics as discussed below. The Fourier transform (FT) of the PE state energy time evolution is shown in Fig. 2(d). The main peaks at the low frequencies originate from the bending and torsional phonons of P3HT, which are responsible for the changes in the PE state. The smaller peak around 1400 cm^{-1} is present in all three junctions and it corresponds to the conjugated C–C bonds in both P3HT and fullerenes.

The energy evolutions during the MD simulations are shown in Fig. 3 where the HOMO and LUMO levels of P3HT fluctuate considerably. In contrast to the energy diagram at 0 K, P3HT LUMO or the PE state (red) overlaps with the fullerene levels (black), leading to the delocalization of the PE state and interfacial ET. On the other hand, P3HT HOMO (blue) is inside the band gap, and well separated from the fullerene levels. The variation in the fullerene energy levels is relative small due to the rigidity of the molecule. The degenerate energy levels of C_{60} and Li@C_{60} have a small splitting during the MD, while the fourth to the seventh PCBM energy levels span a rather large energy range. These levels overlap very well with P3HT LUMO, thus, it is expected that P3HT/PCBM should have very efficient interfacial ET.

The interfacial electron dynamics can be characterized by the time-dependence of fractional ET as shown in Fig. 3. The total ET fraction curve (red) is fitted to the following equation:[18]

$$\mathrm{ET}(t) = \mathrm{ET_f}\{1 - \exp[-(t + t_0)/\tau]\}, \quad (1)$$

in order to estimate the elapsed time (τ) and final amount ($\mathrm{ET_f}$) of interfacial ET, summarized in Table I. t_0 (the intercept of the time axis) is the elapsed time corresponding to the pretransferred amount.

For all three systems, the interfacial ET takes place in a time-scale of ~70 fs, which is consistent with the experimentally observed upper-bound of 200 fs.[7,10] The final amount of total ET is 0.67, 0.41, and 0.78 e for P3HT/C_{60}, P3HT/Li@C_{60} and P3HT/PCBM, respectively. The least amount of ET in P3HT/Li@C_{60} is due to the charge transfer from Li to C_{60} which reduces the electron affinity of C_{60} and hinders ET from P3HT to C_{60}. For P3HT/C_{60} and P3HT/PCBM, the final amount of the adiabatic contribution is greater than that of the NA contribution. Moreover, for P3HT/C_{60} and P3HT/Li@C_{60}, the adiabatic ET is one order of magnitude faster than the NA ET. As a result, the total ET is dominated by the adiabatic contribution and the total elapsed time is set by the adiabatic time-scale. The NA contribution in P3HT/PCBM is essentially zero. The results can be understood from the energy evolution perspective. As shown in Fig. 3, in P3HT/C_{60}, the PE state overlaps with the C_{60} energy levels for the most of time, leading to ultrafast ET. In P3HT/Li@C_{60}, the PE state overlaps occasionally with the fullerene energy levels, reducing the adiabatic ET; this is because the adiabatic ET requires strong coupling between the donor and acceptor states. On the other hand, the NA ET can take place without the strong coupling as evidenced by a faster NA time-scale in P3HT/Li@C_{60}. In

TABLE I. The fitted τ and $\mathrm{ET_f}$ of P3HT/C_{60}, P3HT/Li@C_{60}, and P3HT/PCBM heterojunctions. The corresponding values of the total, adiabatic and NA contributions are listed separately. The unit of time-scale is femtosecond. There is no result for the NA contribution in P3HT/PCBM because it is vanishingly small.

	P3HT/C_{60}		P3HT/Li@C_{60}		P3HT/PCBM	
	τ	$\mathrm{ET_f}$	τ	$\mathrm{ET_f}$	τ	$\mathrm{ET_f}$
Total	63.9	0.67	67.7	0.41	75.5	0.78
Adiabatic	26.1	0.30	12.0	0.08	60.9	0.55
NA	1034.9		989.2		···	

P3HT/PCBM, the ET is again ultrafast because the PE state overlaps with the fullerene levels for the entire time. The excellent energy overlap in P3HT/PCBM stems from the broader energy distribution (0.5 eV) of PCBM thanks to its lower symmetry. The result of the greater ET in P3HT/PCBM is in contradiction with the speculation of Kanai *et al.*[12] the contradiction is mainly due to the fact that their conclusion was based on the equilibrium electronic structure analysis at 0 K, which does not take into consideration of the energy fluctuations at finite temperatures. The interfacial exciton dissociation at finite temperatures is under investigation by combining MD and time-dependent DFT calculations.

Finally, we have also simulated the backward ET from the fullerene conduction band edge to P3HT HOMO. For the three junctions, the final population on P3HT HOMO is less than 0.0004 within 200 fs, which suggests that the backward transfer process is in the nanosecond range, much slower than the forward process and is consistent with the experimental estimate of 0.8 ns.[7,11] In addition, we find that the final amount of the backward ET in P3HT/PCBM is an half of that in the other two junctions, which may arise from the larger average energy difference between PCBM LUMO and P3HT HOMO, as shown in Fig. 3.

To summarize, the *ab initio* NA MD simulations are carried out to study the interfacial electronic structure and dynamics in P3HT/C_{60}, P3HT/Li@C_{60}, and P3HT/PCBM heterojunctions. All three junctions allow ultrafast ET with a time-scale of ~70 fs. In P3HT/C_{60} and P3HT/PCBM, the adiabatic ET is the dominant process. For the backward ET, the time-scale is in nanoseconds and P3HT/PCBM backward ET is slower than the two other junctions.

This work was supported by NSF under Grant Nos. DMR-1035480 (Solar) and DMR-0958596 (MRI).

[1]G. Yu and A. J. Heeger, J. Appl. Phys. **78**, 4510 (1995).
[2]J. J. M. Halls, C. A. Walsh, N. C. Greenham, E. A. Marseglia, R. H. Friend, S. C. Moratti, and A. B. Holmes, Nature (London) **376**, 498 (1995).
[3]W. L. Ma, C. Y. Yang, X. Gong, K. Lee, and A. J. Heeger, Adv. Funct. Mater. **15**, 1617 (2005).
[4]G. Li, V. Shrotriya, J. S. Huang, Y. Yao, T. Moriarty, K. Emery, and Y. Yang, Nat. Mater. **4**, 864 (2005).
[5]P. Schilinsky, C. Waldauf, and C. J. Brabec, Appl. Phys. Lett. **81**, 3885 (2002).
[6]M. Campoy-Quiles, T. Ferenczi, T. Agostinelli, P. G. Etchegoin, Y. Kim, T. D. Anthopoulos, P. N. Stavrinou, D. D. C. Bradley, and J. Nelson, Nature Mater. **7**, 158 (2008).
[7]I. W. Hwang, D. Moses, and A. J. Heeger, J. Phys. Chem. C **112**, 4350 (2008).
[8]S. Trotzky, T. Hoyer, W. Tuszynski, C. Lienau, and J. Parisi, J. Phys. D: Appl. Phys. **42**, 055105 (2009).
[9]D. E. Motaung, G. F. Malgas, C. J. Arendse, S. E. Mavundla, C. J. Oliphant, and D. Knoesen, Sol. Energy Mater. Sol. Cells **93**, 1674 (2009).
[10]J. Piris, T. E. Dykstra, A. A. Bakulin, P. H. M. van Loosdrecht, W. Knulst, M. T. Trinh, J. M. Schins, and L. D. A. Siebbeles, J. Phys. Chem. C **113**, 14500 (2009).
[11]J. M. Guo, H. Ohkita, H. Benten, and S. Ito, J. Am. Chem. Soc. **132**, 6154 (2010).
[12]Y. Kanai and J. C. Grossman, Nano Lett. **7**, 1967 (2007).
[13]Y. Kanai, Z. G. Wu, and J. C. Grossman, J. Mater. Chem. **20**, 1053 (2010).
[14]C. F. N. Marchiori and M. Koehler, Synth. Met. **160**, 643 (2010).
[15]D. M. Huang, R. Faller, K. Do, and A. J. Moule, J. Chem. Theory Comput. **6**, 526 (2010).
[16]C. F. Craig, W. R. Duncan, and O. V. Prezhdo, Phys. Rev. Lett. **95**, 163001 (2005).
[17]W. Stier and O. V. Prezhdo, J. Phys. Chem. B **106**, 8047 (2002).
[18]W. R. Duncan, W. M. Stier, and O. V. Prezhdo, J. Am. Chem. Soc. **127**, 7941 (2005).
[19]Z. Li, X. Zhang, and G. Lu, J. Phys. Chem. B **114**, 17077 (2010).
[20]G. Kresse and J. Hafner, Phys. Rev. B **47**, 558 (1993).
[21]G. Kresse and J. Furthmuller, Phys. Rev. B **54**, 11169 (1996).